J Solid State Electrochem (2012) 16:1133–1140
DOI 10.1007/s10008-011-1503-8

ORIGINAL PAPER

A new amperometric H_2O_2 biosensor based on nanocomposite films of chitosan–MWNTs, hemoglobin, and silver nanoparticles

Yancai Li · Yuanjun Li · Yiyun Yang

Received: 1 April 2011 / Revised: 15 June 2011 / Accepted: 3 July 2011 / Published online: 22 July 2011

Abstract A new H_2O_2 biosensor was fabricated on the basis of nanocomposite films of hemoglobin (Hb), silver nanoparticles (AgNPs), and multiwalled carbon nanotubes (MWNTs)–chitosan (Chit) dispersed solution immobilized on glassy carbon electrode (GCE). The immobilized Hb displayed a pair of well-defined and reversible redox peaks with a formal potential ($E^{\theta'}$) of −22.5 mV in 0.1 M pH 7.0 phosphate buffer solution. The apparent heterogeneous electron transfer rate constants (k_s) in the Chit–MWNTs film was evaluated as 2.58 s^{-1} according to Laviron's equation. The surface concentration (Γ^*) of the electroactive Hb in the Chit–MWNTs film was estimated to be $(2.48\pm0.25)\times10^{-9}$ mol cm^{-2}. Meanwhile, the Chit–MWNTs/Hb/AgNPs/GCE demonstrated excellently electrocatalytical ability to H_2O_2. Its apparent Michaelis–Menten constant (K_M^{app}) for H_2O_2 was 0.0032 mM, showing a good affinity. Under optimal conditions, the biosensors could be used for the determination of H_2O_2 ranging from 6.25×10^{-6} to 9.30×10^{-5} mol L^{-1} with a detection limit of 3.47×10^{-7} mol L^{-1} (S/N=3). Furthermore, the biosensor possessed rapid response to H_2O_2 and good stability, selectivity, and reproducibility.

Keywords Multiwalled carbon nanotubes · Chitosan · Hemoglobin · Silver · Nanoparticles · Biosensor

Y. Li (✉) · Y. Li · Y. Yang
Chemistry Department, Zhangzhou Normal University,
Fujian, Zhangzhou 363000, People's Republic of China
e-mail: liyancai2000@yahoo.com.cn

Introduction

Hydrogen peroxide (H_2O_2) is an essential mediator in food, pharmaceutical, clinical, industrial, and environmental analyses [1], so it is of great significance to determine the hydrogen peroxide rapidly, accurately, and conveniently. Various methods for H_2O_2 determination have been developed, such as titrimetry, photometry, chemiluminescence, and electrochemistry. However, it must be pointed out that these centralized and sophisticated analytical systems need complicated process and expensive instruments. Therefore, much attention has been paid to the development of high-performance hydrogen peroxide biosensors.

Hemoglobin (Hb), a molecule with four electroactive iron hemes and a molar mass of approximately 64,500 g mol^{-1}, can electrocatalyze the reduction of H_2O_2. Hb also has many advantages such as commercial availability, moderate cost, and its known and documented structure besides its intrinsic peroxidase activity. Consequently, it is possible to employ Hb to construct the hydrogen peroxide biosensors. However, the electroactive center of Hb was embedded deeply in the protein molecular structure, thus the direct electron transfer (DET) between enzyme and the electrode surface was often slow due to its extended 3-D structure, the unfavorable orientation and its strong adsorption onto the electrode surface. Many modifiers had been used to enhance the DET rate between the electrode surface and the prosthetic groups in the proteins, such as surfactants [2], polymers [3–6], inorganic materials [7, 8], metal nanoparticles [9–12], quantum dots [13, 14], and some solvents [15].

Carbon nanotubes (CNTs), a new class of nanomaterial, have been widely employed in biosensors due to its unique mechanical and electrical properties since their discovery in 1991 by Iijima [16]. CNTs can shorten the distance between the redox active center of proteins and the electrode surface,

so the direct electron transfer become more easily. Several CNTs-based unmediated H_2O_2 biosensors have been reported [17–19]. However, due to the existence of van der Waals force, the solubility and dispersion of CNTs appear quite difficult. Several solvents have been used to disperse the CNTs, such as acetone [20], dehexadecyl hydrogen phosphate [21], and *N*,*N*-dimethylformamide [22] etc. But the biological incompatibility of these solvents limited the development of their applications [23]. Zhang et al. has constructed a dehydrogenase biosensor based on the solubilization of CNTs in chitosan solution [24]. Chitosan, the principal derivative of chitin, is a copolymer of *N*-acetyl-D-glucosamine and D-glucosamine. It possesses distinct chemical and biological properties [25]. In its linear polyglucosamine chains of high molecular weight, chitosan has reactive amino and hydroxyl groups, amenable to chemical modifications [26, 27]. Additionally, amino groups make chitosan a cationic polyelectrolyte (pKa≈ 6.5) and soluble in aqueous acidic media at pH<6.5. The solubility in acidic solutions and aggregation with polyanions impart chitosan with excellent gel-forming properties. Therefore, we chose chitosan as the solvent to disperse CNTs. However, chitosan not only used as a solubilizing agent for multiwalled carbon nanotubes (MWNTs), also served as an effective enzyme immobilization matrix.

In order to optimize the performance of biosensors and achieve the DET between protein and electrode more conveniently, the research interest has extended to modify CNTs with nanomaterials. The introduction of nanomaterials has overcome the shortcomings of conventional biosensor, enhanced the sensitivity of current response of biosensor effectively, and provided infinite imagination for the development of biosensor. Several metal nanoparticles such as Pd [28], Ag [29], Pt [30, 31], and Au [32] have successfully been introduced into the CNTs. Owing to the quantum characteristics of small granule diameter, large specific surface area, and the ability to quickly transfer electron, silver nanoparticles have been widely used to the DET of protein. It is noted that silver nanoparticles have successfully been used in Hb immobilization and the direct electron transfer has been obtained. Because of the good biocompatibility and catalytic activity, silver nanoparticles can provide an environment similar to the native environment of Hb and be used to immobilize Hb for its direct electrochemistry. However, few studies about H_2O_2 biosensors based on the chitosan (Chit)–MWNTs/silver nanoparticles (AgNPs)–Hb nanocomposite film were reported previously.

In this paper, we successfully fabricated a new H_2O_2 biosensor based on the nanocomposite films of Chit–MWNTs/Hb/AgNPs. The MWNTs–chitosan dispersed solution was taken as the immobilization matrix. Silver nanoparticles and Hb were immobilized on the glassy carbon electrode (GCE) surface with the Chit–MWNTs composite film. We achieved favorable DET signal of Hb in the nanocomposite film. We also characterized the electrocatalytic properties of the nanocomposite film. It demonstrated excellently electrocatalytical ability toward the reduction of H_2O_2 and can be used as a H_2O_2 biosensor. Furthermore, the biosensor displayed high sensibility, good reproducibility, and long-term stability.

Experimental

Reagents

Bovine red cells hemoglobin was obtained from Worthington Biochemical Corporation and used as received. The multiwalled carbon nanotubes (MWNTs, >95% purity) were purchased from Shenzhen nanoport Co. Ltd. Chitosan (deacetylation, >95%) was obtained from Sanland Chemical Co. Ltd. Both trisodium citrate dihydrate and sodium borohydride were purchased from Sinopharm Chemical Reagent Co. Ltd. Silver nitrate was from Shantou Xilong chemical factory Guangdong. Stock solutions of H_2O_2 were freshly diluted from 30% solution (purchased from Shantou Xilong Chemical Co. Ltd). Of the phosphate buffer solutions (PBS), 0.1 M with various pH values were prepared by mixing stock standard solutions of Na_2HPO_4 and NaH_2PO_4. The supporting electrolyte was 0.1 M KCl. A stock solution of 3 mg/mL Hb was freshly prepared with a phosphate buffer solution (pH 7.32). A chitosan solution (0.8 wt.%) was prepared by dissolving 0.024 g chitosan in 3 mL acetic acid (*v*/*v*, 1%). All other chemicals were of analytical grade and were used without further purification. All solutions were made up with double-distilled water.

Apparatus

UV-visible (UV-Vis) spectra were recorded on a GBC Cintra 10_e UV-Visible spectrameter. The electrochemical experiments were carried out with a CHI 650 C electrochemical workstation (CH Instruments, USA) with a conventional three-electrode cell. The modified or unmodified glassy carbon electrode was used as the working electrode. The Pt wire and Ag/AgCl (3.0 M KCl) electrode were used as the counter and reference electrodes, respectively. Cyclic voltametric measurements were performed in a static cell while amperometric experiments were carried out in a stirred system. All solutions were purged with high-purity nitrogen for at least 20 min prior to experiments and a nitrogen environment was then kept over the solution in the cell. All experiments were performed at a temperature of 20±2°C. Aliquots of hydrogen peroxide solution were added successively to the solution in amperometric experi-

ments. Current time data were recorded after a steady-state current had been achieved.

Preparation of AgNPs

All glassware used in the procedures was firstly washed with freshly prepared HNO_3/HCl (1:3, *v*/*v*), then rinsed thoroughly with double-distilled water and dried prior to use. Silver nanoparticles were prepared according to the literature [33] by using sodium citrate and sodium borohydride to reduce silver nitrate in a mixing solution. $AgNO_3$ and Na_3citrate solutions needed were filtered through a 22 μm microporous membrane filter prior to use. In brief, 1 mL of $AgNO_3$ was added to 90 mL of double-distilled water. After 1 min of stirring, 2 mL of sodium citrate (1 wt.%) was added. One minute later, 1 mL of fresh 0.075% $NaBH_4$ (prepared in the 1% sodium citrate solution) was added. The solution was stirred for an additional 5 min, poured into a brown glass bottle and stored at 4°C. The electronic absorption peak of the silver nanoparticles prepared is about 390 nm in the visible region. The average nanoparticle diameter is 8±2.4 nm as measured by transmission electron microscopy (not shown here).

Preparation of Chit–MWNTs/Hb/AgNPs/GC electrode

Glassy carbon electrode (3 mm diameter) were polished with 1.0, 0.3, and 0.05 μm alumina slurry, respectively, and then ultrasonically cleaned in ethanol and double-distilled water for about 1 min, respectively. Then, GCE was cycled in the potential range between 0.4 and −0.4 V at 100 mV/s for two cycles in 6 mL of 5 mM $K_3[Fe(CN)_6]$. Upon putting 6 mg of MWNTs into 3 mL of a chitosan solution (0.8wt.%), ultrasonic agitation for a few minutes gave a black suspension. Hb solution was obtained by dissolving 9 mg of Hb in 3 mL of 0.1 M pH 7.32 PBS, and the AgNPs were used as prepared. Then, 20-μL mixture of Hb and AgNPs (*v*/*v*=1:1) was dropped onto the surface of a cleaned glassy carbon electrode with a microsyringe and allowed to dry at 4°C for 24 h. After the GCE was cooled, it was smeared evenly with 20 μL of a chitosan–MWNTs (0.8 wt.%) solution by a microsyringe, and then dried at a temperature of 4°C for another 24 h. The solvent was allowed to evaporate before use. The final electrode is taken as the Chit–MWNTs/Hb/AgNPs/GCE. The similar procedures were employed to fabricate the Chit–MWNTs/AgNPs/GCE and Chit–MWNTs/Hb/GCE. All resulting electrodes were stored at 4°C when not in use.

A 0.1 M phosphate buffer solution (pH 7.0) was used as supporting electrolyte for the determination of hydrogen peroxide. Before and after every measurement, the Chit–MWNTs/Hb/AgNPs/GCE was activated by successive cyclic voltammetric sweeps between −0.3 and 0.5 V at 100 mV/s in phosphate buffer solution (pH 7.0).

Results and discussion

UV-Vis characterization

The position of the Soret absorption band of heme can provide information about the possible denaturation of heme protein, especially of that conformational change in the heme group region. As seen from Fig. 1, the dry film on quartz slides gave a Soret band of Hb at 410 nm (Fig. 1b), the same position as that in hemoglobin solution (Fig. 1a). It also agrees well with the literature [34] reported previously. The accordance indicates that the heme status of the entrapped Hb in the Chit–MWNTs/Hb/AgNPs composite films retains its natural structure and not denatured.

Direct electrochemistry of Hb

Figure 2 shows the cyclic voltammograms of different electrodes in 0.1 M pH 7.0 PBS at 100 mV/s. As shown in Fig. 2d, the Chit–MWNTs/Hb/AgNPs GCE exhibited a couple of stable and well-defined redox peaks at 13 and −58 mV at 100 mV/s, with the formal potential ($E^{\theta'}$) of −22.5 mV, while no peak was observed at either bare GCE (Fig. 2a) or Chit–MWNTs/AgNPs/GCE (Fig. 2b), which only displayed a small background current. Obviously, the response of Chit–MWNTs/Hb/AgNPs/GCE was ascribed to the redox of the electroactive center of the immobilized Hb. The presence of silver nanoparticles resulted in a slight decrease of the background current. When Hb was immobilized in Chit–MWNTs–GCE without

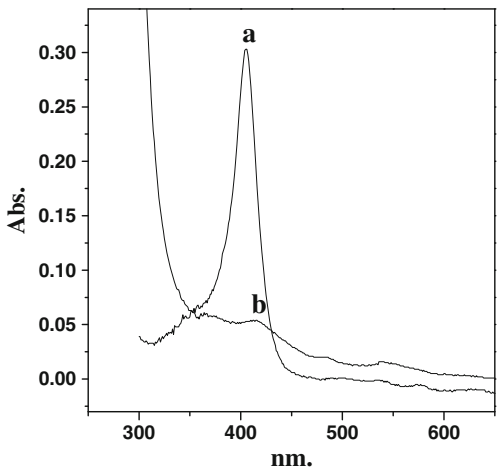

Fig. 1 UV–Vis absorption spectra of *a* pure hemoglobin solution (3 mg/mL) and *b* the Chit–MWNTs/Hb/AgNPs film on quartz slides

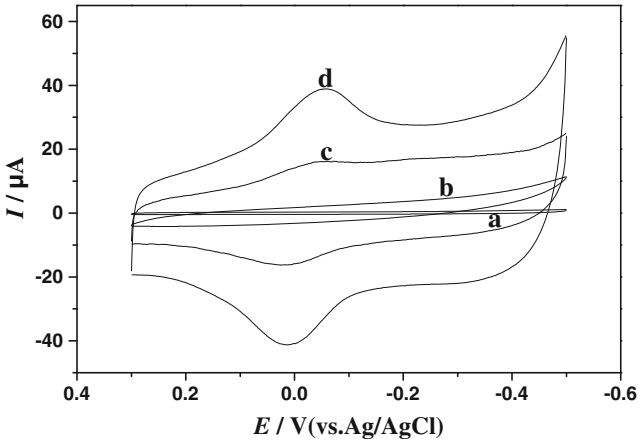

Fig. 2 Cyclic voltammograms of *a* bare GCE, *b* Chit–MWNTs/AgNPs/GCE, *c* Chit–MWNTs/Hb/GCE, and *d* Chit–MWNTs/Hb/AgNPs/GCE in 0.1 M pH 7.0 PBS at 100 mV/s

the presence of AgNPs, the Chit–MWNTs/Hb/GCE showed a lower and less reversible faradic response (Fig. 2c). However, the redox peaks were asymmetric and the oxidation peak current was much larger than its reduction peak current. The presence of AgNPs resulted in a great increase of reduction peak current, which was probably ascribed to the electrostatic interaction between AgNPs and Hb (Fig. 2d). In addition, the response of Chit–MWNTs/Hb/AgNPs/GCE showed about 2.2 times larger than that of Chit–MWNTs/Hb-modified GCE, indicating Chit–MWNTs–AgNPs play an important role in maintaining the biological activity of Hb and facilitating the electron transfer between Hb and the electrode surface.

Figure 3 shows the cyclic voltammograms of the Chit–MWNTs/Hb/AgNPs modified glassy carbon electrode in 0.1 M PBS (pH 7.0) at different scan rates. The voltammograms have well-defined redox peaks and the peak currents

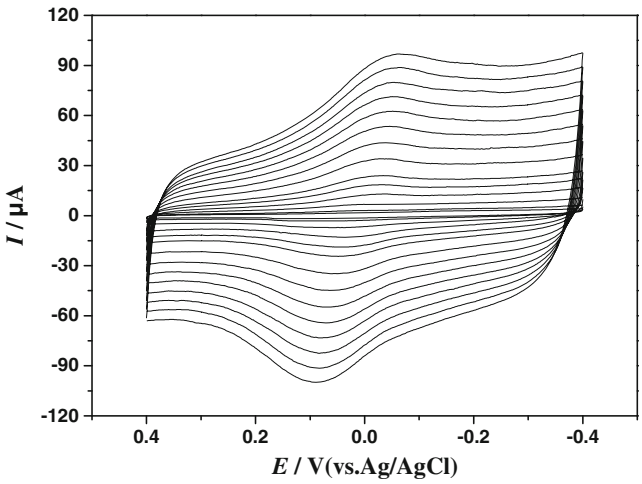

Fig. 3 Cyclic voltammograms of Chit–MWNTs/Hb/AgNPs/GCE in pH 7.0 PBS at 10, 25, 50, 75, 100, 150, 200, 250, 300, 350, 400, 450, and 500 mV/s (from inner to outer)

increased gradually with the increase of the scan rate. It can also be seen from Fig. 4, the redox peak currents increased linearly with the scan rate in the scan rate range of 10–500 mV/s, which characterized as surface-controlled electrochemical process. The linear regression equations expressed as follows: I_{pc} $(A)=3.79+0.19v$ (V/s) (R=0.9986); I_{pa} $(A)=-3.89–0.20v$ (V/s; R=0.9990). Moreover, the cathodic peak currents were almost the same as the corresponding anodic peak currents and the peak potentials nearly did not change with increasing scan rate, indicating that all the electroactive ferric hemoglobin [Hb–Fe(III)] in the film is reduced to ferrous hemoglobin [Hb–Fe(II)] on the forward scan to negative potentials and that the Hb–Fe(II) produced is reoxidized to Hb–Fe(III) on the reverse scan.

The surface coverage(Γ^*) was calculated from integration of the reduction peak of the cyclic voltammograms according to $\Gamma = Q/nFA$, where Q is the charge involved in the reaction, n is the number of electron transferred, F is Faraday constant, and A is the effective area of GCE. The surface concentration of electroactive Hb (Γ^*) was estimated to be $(2.48\pm0.25)\times10^{-9}$ mol cm^{-2} of the Chit–MWNTs/Hb/AgNPs/GCE, which was larger than the theoretical monolayer coverage of Hb (1.89 ± 10^{-11} mol cm^{-2}) [35] on the basis of the crystallographic dimensional structure of Hb and assuming that the biomolecule adopts an orientation with the long axis parallel to the electrode surface. Meanwhile, this value is higher than that reported in hemoglobin-CdTe-$CaCO_3$@Polyelectrolytes 3D Architecture [36] or Mb/Gel/GC film [37], which could be ascribe to the good biocompatibility of chitosan and the large surface area of silver nanoparticles and available orientation of Hb in Chit–MWNTs/Hb/AgNPs/GCE.

The relationship of the peak potentials with scan rate was further constructed, which could be used for the calculation of the electrochemical parameters. When $n\Delta E_p$>200 mV, the direct electron transfer rate constant

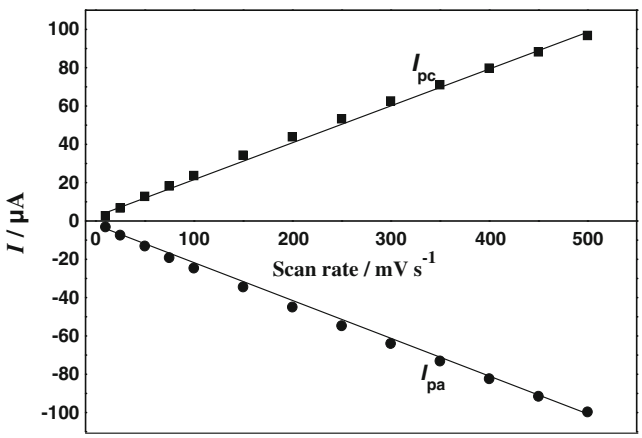

Fig. 4 Relationship between scan rates and the anodic and cathodic peak currents of Chit–MWNTs/Hb/AgNPs/GCE in 0.1 M pH 7.0 PBS

(k_s) of the immobilized Hb on the Chit–MWNTs/Hb/AgNPs/GCE can be obtained by Laviron's equations [38]:

$$\log k_s = \alpha\log(1-\alpha) + (1-\alpha)\log\alpha - \log(RT/nFv) - \alpha(1-\alpha)nF\Delta E_p/2.3RT$$

where, α is the electron transfer coefficient, n is the electron transfer number, k_s is the apparent heterogeneous electron transfer rate constant, v is the scan rate, ΔE_p is peak potential separation, and F is the Faraday's constant. Experimental results showed that the scan rate in the range of 10–500 mV/s did not affect the k_s value. Taking the charge–transfer coefficient α of 0.5, at a scan rate of 100 mV/s, the k_s of the immobilized Hb on the Chit–MWNTs/Hb/AgNPs/GCE was estimated to be 2.58 s^{-1}. The value was much larger than the one obtained for Hb immobilized by the polyelectrolyte–surfactant polymer and carbon nanotubes self-assembled glassy carbon electrode (0.41 s^{-1}) [39], Hb immobilized on an Au colloid–cysteamine-modified gold electrode of 0.49 s^{-1} [40]. The fast electron transfer rate resulted from the strong interaction between Hb molecules and AgNPs. Furthermore, chitosan can provide a good biocompatibility for Hb and MWNTs could facilitate the electron transfer.

CV responses in the reduction of H_2O_2

The electrocatalytic response of the Chit–MWNTs/Hb/AgNPs/GCE toward H_2O_2 was also investigated. Figure 5 displays the cyclic voltammograms obtained for the hydrogen peroxide biosensor in 0.1 M pH 7.0 PBS containing various concentration of H_2O_2 in absence of oxygen. The catalytic response of the biosensor toward hydrogen peroxide can be seen clearly. With the addition of 0.1 M H_2O_2, the reduction peak current increased obviously while the oxidation peak current decreased (Fig. 5b). The reduction current increased linearly with the concentration of H_2O_2 in solution, as shown in the inset of Fig. 5. However, no similar cathodic peak corresponding to the reduction of H_2O_2 was observed on GCE, Chit–MWNTs/AgNPs/GCE under the same condition. So, we can conclude that Hb immobilized in composite membrane shows good catalytic ability to hydrogen peroxide.

Selection of the applied potential

Figure 6 shows the influence of applied potential on the amperometric determination of constant concentration (0.1 M) H_2O_2 in the range from 0.1 to −0.32 V. As seen from Fig. 6, the catalytic current increased sharply from 0.1 to −0.3 V, and reached the maximum at −0.3 V, then slightly decreased at more negative potentials than −0.3 V. The catalytic current of the sensor achieved a platform when the potential arrived at −0.3 V while the current began to decrease after −0.32 V. Therefore, a constant potential of −0.3 V was adopted to get the maximum sensitivity, and we chose −0.3 V as the applied potential for detecting H_2O_2 in the amperometric experiment.

Amperometric response to hydrogen peroxide

Figure 7 shows a current time plot of Chit–MWNTs/Hb/AgNPs/GCE at applied potential of −0.3 V upon successive additions of aliquot H_2O_2 to pH 7.0 phosphate buffer solutions. As H_2O_2 was added into the stirring buffer solution with regular speed, the modified electrode could

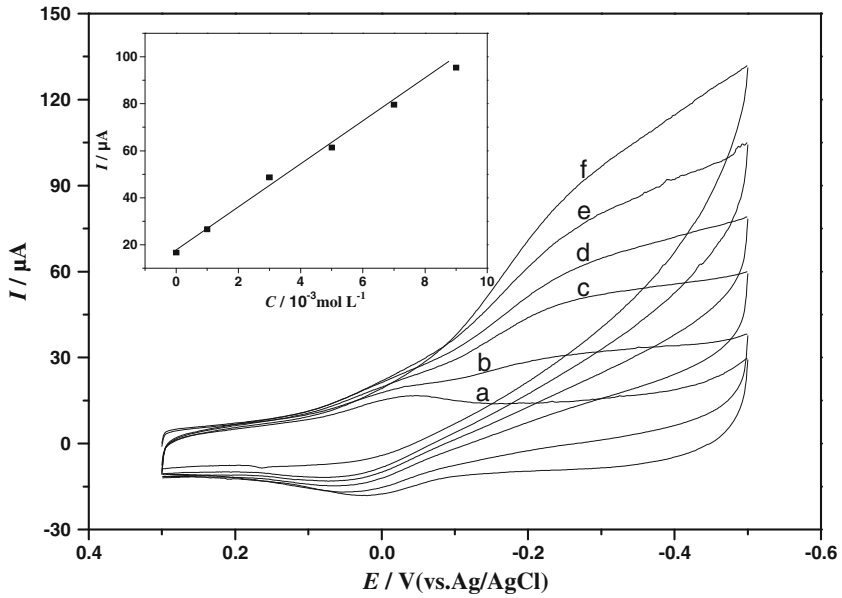

Fig. 5 Cyclic voltammograms of Chit–MWNTs/Hb/AgNPs/GCE in 0.1 M pH 7.0 PBS containing H_2O_2 *a* 0 mM, *b* 1 mM, *c* 3 mM, *d* 5 mM, *e* 7 mM, *f* 9 mM. *Inset* plot of catalytic peak current vs. the concentration of H_2O_2

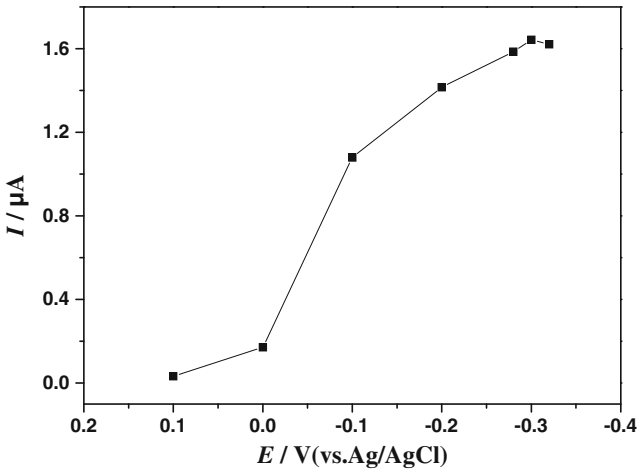

Fig. 6 Effect of applied potential on the response of the sensor in the presence of 0.1 M H_2O_2 in 0.1 M pH 7.0 phosphate buffer solution

attain the steady-state current within less than 5 s, indicating a fast amperometric response to the reduction of H_2O_2. For the composite film, the amperometric response was linearly within the concentration range from 6.25×10^{-6} to 9.30×10^{-5} mol L^{-1}, the linearly regression equation was I (μA)=5.38 +0.034 [H_2O_2] (M), with a correlation coefficient of 0.998 (n=11). The detection limit of biosensor was estimated to be 3.47×10^{-7} mol L^{-1} at S/N of 3, which was lower than that of carbon paste electrode containing hemoglobin and colloidal gold [41], indicating an excellent improvement in sensitivity of the H_2O_2 biosensors. What's more, the detection limit was also lower than that of hydrogen peroxide biosensors such as poly (ε-caprolactone) film electrode [42], hemoglobin on carbonized titania nanotubes-modified GCE [43], indicating that the proposed biosensor could be used for detecting of the lower concentration of H_2O_2. The lower detection limit could be ascribed to the high loading of hemoglobin on the electrode surface via the presence of AgNPs and MWNTs and their ability to promote the direct electron transfer.

The apparent Michaelis–Menten constant (K_M^{app}), which provided to be an indication of the enzyme substrate kinetics, was calculated from the electrochemical version of the Lineweaver–Burk equation [44]

$$1/I_{ss} = 1/I_{max} + K^{app}{}_M/I_{max}C$$

where, I_{SS} is the steady-state current after the addition of substrate, which can be obtained from amperometric experiments, I_{max} is the maximum current under saturated substrate condition, and C is the bulk concentrate of the substrate. The value of the apparent Michaelis–Menten constant (K_M^{app}) can be calculated from the slope (K_M^{app}/I_{max}) and the intercept ($1/I_{max}$) for the plot of the reciprocals of the steady-state current (I_{SS}) versus H_2O_2 concentration (C). By analysis of the steady-state current and the H_2O_2 concentration, the apparent Michaelis–Menten constant could be calculated as 0.0032 mM, which was much lower than that of previous reports such as hemoglobin at a carbon nanotube electrode [45], hemoglobin immobilized on multiwall carbon nanotubes and gold colloidal nanoparticles films [46] and hemoglobin in a hexagonal mesoporous silica matrix [47]. The lower value of K_M^{app} indicates that Hb immobilized in Chit–MWNTs/Mb/AgNPs/GCE film retains its bioactivity and shows high electrocatalytic efficiency toward the reduction of H_2O_2.

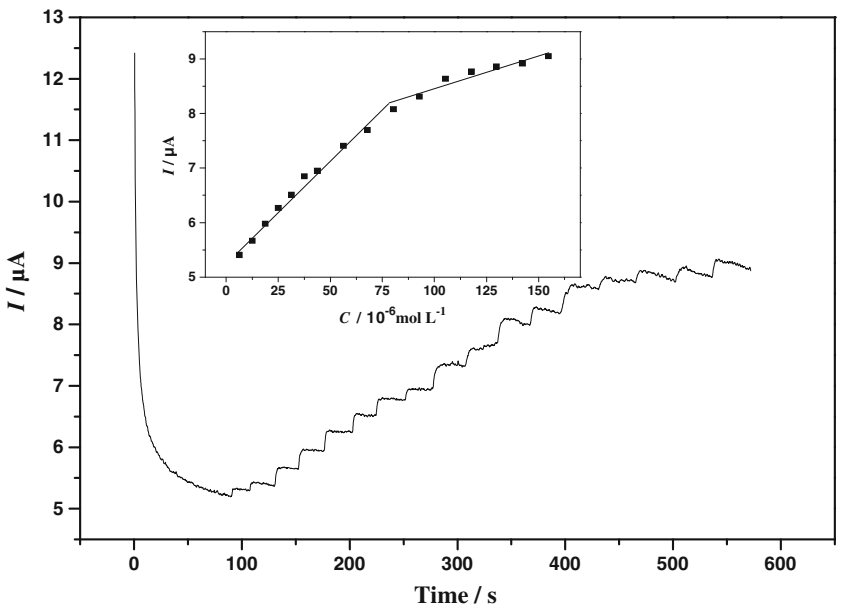

Fig. 7 Amperometric response of Chit–MWNTs/Hb/AgNPs modified GCEs at −0.3 V upon successive additions of 20 μL 6.25 mM H_2O_2 to 5.0 mL 0.1 M pH 7.0 PBS

Stability, reproducibility, and selectivity of the biosensors

The proposed biosensor showed high stability. When the 50 continuous cyclic scans was carried out in the potential range from 0.3 to −0.5 V at a scan rate of 50 mV/s, only 5% decrease of the initial response is observed. On the other hand, a storage period of a week in 0.1 M pH 7.0 PBS at 4°C was investigated when not in use. During the first 3 days, the response current had about 5% decreases and in the next 2 weeks the current response decreased about 8.7% of its initial response, and 13% for 1 month. The relative standard deviation was 3.5% for nine successive measurements at 6.25 mM hydrogen peroxide, showing the proposed biosensor possesses a good reproducibility.

In order to examine the selectivity of the biosensor, we carried out interference measurement towards the electrochemical reduction of H_2O_2 in the presence of some potentially coexisting compounds, such as dopamine (DA), uric acid (UA), and ascorbic acid (AA). As for the proposed biosensor, amperometric steady-state curve has also been carried out at −0.3 V for successive addition of DA, UA and AA to electrochemical cell, the catalytic current of H_2O_2 was used to evaluate the interference of those interfering substances. Compared with equal amount of H_2O_2 at this potential, the amperometric responses of DA, UA, and AA were very low. When 1.0 mmol L^{-1} AA, UA, and DA were added to PBS containing 0.1 mmol L^{-1} H_2O_2, the current response for amperometric determination of H_2O_2 increased about 5.25%, 3.78%, and 2.46%, respectively. The results also indicate that the biosensor has better selectivity. We propose that Hb in the Chit–MWNTs/Hb/AgNPs composite film can exhibit a fine peroxidase character and a high catalytic activity to H_2O_2, which makes Hb-based H_2O_2 biosensor have a good selectivity.

Conclusions

In this experiment, we succeeded in preparing a H_2O_2 biosensor based on the Chit–MWNTs and Hb–AgNPs composite films modified glassy carbon electrode. This novel method was simple, convenient, and versatile. The presence of AgNPs and MWNTs had greatly enhanced the direct electron transfer between Hb and the surface of electrode. Chitosan had excellent biocompatibility and could provide a better microenvironment for Hb in the composite membrane. The resulting biosensor exhibited excellent electrocatalytic response to the reduction of H_2O_2 and could be used as an amperometric sensor for the determination of H_2O_2. Moreover, the biosensor possessed good stability and reproducibility.

Acknowledgments This work was supported by the Fujian Provincial Department of Education projects (JA09163) and Graduate students education innovation base funds of Zhangzhou Normal University and Zhangzhou Normal University Research Fund (L20779).

References

1. Wu ZY, Tang YY, Shen GL, Yu RQ (2006) Synthesis and application of novel H_2O_2 fluorescent probe based on the deprotection mechanism. Acta Chim Sin 64:738–742
2. Mimica D, Zagal JH, Bedioui F (2001) Electroreduction of nitrite by hemin, myoglobin and hemoglobin in surfactant films. J Electroanal Chem 497:106–113
3. Liu XJ, Chen T, Liu LF, Li GX (2006) Electrochemical characteristics of heme proteins in hydroxyethylcellulose film. Sens Actuat B-Chem 113:106–111
4. Lu Q, Hu SS (2006) Studies on direct electron transfer and biocatalytic properties of hemoglobin in polytetrafluoroethylene film. Chem Phys Lett 424:167–171
5. Wang B, Dong S (2000) Sol–gel-derived amperometric biosensor for hydrogen peroxide based on methylene green incorporated in Nafion film. Talanta 51:565–572
6. Ma L, Tian YN, Rong ZJ (2007) Direct electrochemistry of hemoglobin in the hyaluronic acid films. J Biochem Biophys Methods 70:657–662
7. Zhao G, Feng JJ, Xu JJ, Chen HY (2005) Direct electrochemistry and electrocatalysis of heme proteins immobilized on self-assembled ZrO_2 film. Electrochem Commun 7:724–729
8. Topoglidis E, Astuti Y, Duriaux F, Gratzel M, Durrant JR (2003) Direct electrochemistry and nitric oxide interaction of heme proteins adsorbed on nanocrystalline tin oxide electrodes. Langmuir 19:6894–6900
9. Zhang JD, Oyama M (2004) A hydrogen peroxide sensor based on the peroxidase activity of hemoglobin immobilized on gold nanoparticles-modified ITO electrode. Electrochim Acta 50:85–90
10. Zhang L, Jiang X, Wang EK, Dong SJ (2005) Attachment of gold nanoparticles to glassy carbon electrode and its application for the direct electrochemistry and electrocatalytic behavior of hemoglobin. Biosens Bioelectron 21:337–345
11. Zhao S, Zhang K, Sun YY, Sun CQ (2006) Hemoglobin/colloidal silver nanoparticles immobilized in titania sol–gel film on glassy carbon electrode:direct electrochemistry and electrocatalysis. Bioelectrochemistry 69:10–15
12. Wang FC, Yuan R, Chai YQ, Tang DP (2007) Probing traces of hydrogen peroxide by use of a biosensor based on mediator-free DNA and horseradish peroxidase immobilized on silver nanoparticles. Anal Bioanal Chem 387:709–717
13. Lu Q, Hu SS, Pang DW, He ZK (2005) Direct electrochemistry and electrocatalysis with hemoglobin in water-soluble quantum dots film on glassy carbon electrode. Chem Commun 20:2584–2585
14. Xu YX, Liang JG, Hu CG, Wang F, Hu SS, He ZK (2007) A hydrogen peroxide biosensor based on the direct electrochemistry of hemoglobin modified with quantum dots. J Biol Inorg Chem 12:421–427
15. Xu YX, Wang F, Chen XX, Hu SS (2006) Direct electrochemistry and electrocatalysis of heme-protein based on *N*,*N*-dimethylformamide film electrode. Talanta 70:651–655
16. Iijima S (1991) Helical microtubules of graphitic carbon. Nature 354:56–58
17. Zhao GC, Zhang L, Wei XW (2004) An unmediated H_2O_2 biosensor based on the enzyme-like activity of myoglobin on multi-walled carbon nanotubes. Anal Biochem 329:160–161

18. Ando Y, Zhao XL, Inoue S, Iijima S (2002) Mass production of multiwalled carbon nanotubes by hydrogen arc discharge. J Crystal Growth 237:1926–1930
19. Zhao GC, Yin ZZ, Zhang L, Wei XW (2005) Direct electrochemistry of cytochrome c on a multi-walled carbon nanotubes modified electrode and its electrocatalytic activity for the reduction of H_2O_2. Electrochem Commun 7:256–260
20. Wu FH, Zhao GC, Wei XW (2002) Electrocatalytic oxidation of nitric oxide at multi-walled carbon nanotubes modified electrode. Electrochem Commun 4:690–694
21. Wu K, Sun Y, Hu S (2003) Development of an amperometric indole-3-acetic acid sensor based on carbon nanotubes film coated glassy carbon electrode. Sens Actuat B-Chem 96:658–662
22. Rouse JH, Lilehei PT, Sanderson J, Siochi EJ (2004) Polymer/single-walled carbon nanotube films assembled via donor-acceptor interactions and their use as scaffolds for silica deposition. Chem Mater 16:3904–3910
23. Zeng Y, Zhu ZH, Wang RX, Lu GH (2005) Electrochemical determination of bromide at a multiwall carbon nanotubes-chitosan modified electrode. Electrochimica Acta 51:649–654
24. Zhang M, Smith A, Gorski W (2004) Carbon nanotube–chitosan system for electrochemical sensing based on dehydrogenase enzymes. anal chem 76:5045–5050
25. Dutta PK, Ravikumar MNV, Dutta J (2002) Chitin and chitosan for versatile applications. J Macromol Sci 42:307–354
26. Tharanathan RN, Kittur FS (2003) Chitin—the undisputed biomolecule of great potential. Crit Rev Food Sci Nutr 43:61–87
27. Kurita K (2001) Controlled functionalization of the polysaccharide chitin. Prog Polym Sci 26:1921–1971
28. Lim SH, Wei J, Lin JY, Li QT, You JK (2005) A glucose biosensor based on electrodeposition of palladium nanoparticles and glucose oxidase onto Nafion-solubilized carbon nanotube electrode. Biosens Bioelectron 20:2341–2346
29. Guo DJ, Li HL (2005) Highly dispersed Ag nanoparticles on functional MWNT surfaces for methanol oxidation in alkaline solution. Carbon 43:1259–1264
30. Yu R, Chen L, Liu Q, Lin J, Tan KL, Ng SC (1998) Nanotubes via chemical modification. Chem Mater 10:718–722
31. Qiang LL, Vaddiraju S, Rusling JF, Papadimitrakopoulos F (2010) Highly sensitive and reusable Pt-black microfluidic array for long term electrochemical sensing. Biosens Bioelectron 26:682–688
32. Liu YQ, Wang TX, Li J, Guo ZX, Dai LM, Zhang DQ, Zhu DB (2003) Self-assembly of gold nanoparticles to carbon nanotubes using a thiol-terminated pyrene as interlinker. Chem Phys Lett 367:747–752
33. Lu YX, Wang QF, Sun JQ, Shen JC (2005) Selective dissolution of the silver component in colloidal Au and Ag multilayers: a facile way to prepare nanoporous gold film materials. Langmuir 21:5179–5184
34. Wang SF, Xie F, Liu GD (2009) Direct electrochemistry and electrocatalysis of heme proteins on SWCNTs-CTAB modified electrodes. Talanta 77:1343–1350
35. Silva CC, Rocha HHB, Freire FNA, Santos MRP, Saboia KDA, Goes JC, Sombra ASB (2005) Hydroxyapatite screen-printed thick films: optical and electrical properties. Mater Chem Phys 92:260–268
36. Cai WY, Feng LD, Liu SH, Zhu JJ (2008) Hemoglobin-CdTe-$CaCO_3$ @polyelectrolytes 3D architecture: fabrication, characterization and application in biosensing. Adv Funct Mater 18:3127–3136
37. Li N, Xu JZ, Yao H, Zhu JJ, Chen HY (2006) The Direct electron transfer of myoglobin based on the electron tunneling in proteins. J Phys Chem B 110:11561–11565
38. Laviron E (1979) General expression of the linear potential sweep voltammogram in the case of diffusionless electrochemical systems. J Electroanal Chem 101:19–28
39. Chen L, Lu GX (2007) Novel amperometric biosensor based on composite film assembled by polyelectrolyte-surfactant polymer, carbon nanotubes and hemoglobin. Sens Actuat B-Chem 121:423–429
40. Gu HY, Yu AM, Chen HY (2001) Direct electron transfer and characterization of hemoglobin immobilized on a Au colloid-cysteamine-modified gold electrode. J Electroanal Chem 516:119–126
41. Liu SQ, Ju HX (2003) Nitrite reduction and detection at a carbon paste electrode containing hemoglobin and colloidal gold. Analyst 128:1420–1424
42. Zheng W, Li J, Zheng YF (2008) An amperometric biosensor based on hemoglobin immobilized in poly (ε-caprolactone) film and its application. Biosens Bioelectron 23:1562–1566
43. Guo CX, Hua FP, Li CM, Shen PK (2008) Direct electrochemistry of hemoglobin on carbonized titania nanotubes and its application in a sensitive reagentless hydrogen peroxide biosensor. Biosens Bioelectron 24:819–824
44. Kamin RA, Wilson GS (1980) Rotating ring-disk enzyme electrode for biocatalysis kinetic studies and characterization of the immobilized enzyme layer. Anal Chem 52:1198–1205
45. Cai C, Chen J (2004) Direct electron transfer and bioelectrocatalysis of hemoglobin at a carbon nanotube electrode. Anal Biochem 325:285–292
46. Chen SH, Yuan R, Chai YQ, Zhang LY, Wang N, Li XL (2007) Amperometric third-generation hydrogen peroxide biosensor based on the immobilization of hemoglobin on multiwall carbon nanotubes and gold colloidal nanoparticles. Biosens Bioelectron 22:1268–1274
47. Dai ZH, Liu SQ, Ju HX, Chen HY (2004) Direct electron transfer and enzymatic activity of hemoglobin in a hexagonal mesoporous silica matrix. Biosens Bioelectron 19:861–867